A new expression of hardening coefficients for fcc-crystal and calibration of the material constants*

LIANG Naigang (梁乃刚), XU Tong (徐 彤)

and WANG Ziqiang (王自强)

(LNM, Institute of Mechanics, Chinese Academy of Sciences, Beijing 100080, China)

Received November 12, 1994

Abstract In order to describe the effect of latent hardening on the macro-plastic behavior of fcc-crystal, a new expression for hardening coefficient is proposed in which there are 12 material constants, each having clear physical meaning. And a method of material constant calibration is suggested and used to determine the material constants of copper and aluminum crystal. The simulated load-elongation curves along various crystallographic orientations are comparable with the experimental ones.

Keywords: latent hardening, hardening law, material constant calibration.

The rigorous geometric and kinematic descriptions of crystal plastic deformation were formulated by Hill[1] in 1966 and Hill and Rice[2] in 1972. Since then the study on the theoretical framework of the crystal constitutive relation has made much headway. Whether the crystal plasticity theory has practical applications largely depends upon the establishment of an appropriate expression of the crystal hardening law. Following the pioneering work of Taylor and Elam, Asaro proposed a hyperbolic hardening function with 4 material constants and used it to analyze the formation of shear bands in crystal[3]; Bassani[4] reexamined the activating condition of the secondary slip systems and argued that the main effect of latent hardening is not to heighten the systems' critical resolved stress but to increase their tangent shear moduli when they are activated. However, there are still considerable discrepancies between the theoretical predictions and the experimental results. Thus this effect needs to be more accurately formulated. Moreover, as the functional relation between experimental curves of crystal and its materials is very complex and implicit, how to determine the material constants poses another outstanding question. This paper attempts to establish a new hardening expression of fcc-crystal and presents a method for calibration of material constants.

Here we first quote a few important formulae of crystal plasticity directly from ref. [3]. Let the normal vector of the αth slip system be $\boldsymbol{n}^{(\alpha)}$ and the vector in the sliding direction be $\boldsymbol{m}^{(\alpha)}$, either of which is initially a unit vector and remains unchanged during

* Project supported by the National Natural Science Foundation of China.

plastic deformation. The symmetrical and unsymmetrical orientation tensors are defined as

$$\boldsymbol{P}^{(\alpha)}=\frac{1}{2}(\boldsymbol{m}^{(\alpha)}\otimes\boldsymbol{n}^{(\alpha)}+\boldsymbol{n}^{(\alpha)}\otimes\boldsymbol{m}^{(\alpha)}) \text{ and } \boldsymbol{W}^{(\alpha)}=\frac{1}{2}(\boldsymbol{m}^{(\alpha)}\otimes\boldsymbol{n}^{(\alpha)}-\boldsymbol{n}^{(\alpha)}\otimes\boldsymbol{m}^{(\alpha)}). \tag{1}$$

With $\dot{\gamma}^{(\alpha)}$ and $\dot{\tau}^{(\alpha)}$ denoting the sliding shear rate and resolved shear stress rate, respectively, the macro plastic strain rate will be

$$D^{\mathrm{P}}=\sum_{\alpha=1}^{N}\dot{\gamma}^{(\alpha)}\boldsymbol{P}^{(\alpha)}. \tag{2}$$

Letting

$$B^{(\alpha)}=\boldsymbol{W}^{(\alpha)}\cdot T-T\cdot\boldsymbol{W}^{(\alpha)}, \tag{3}$$

where T is Kirchhoff stress, the elastic strain rate and resolved shear stress rate will be

$$D^{\mathrm{e}}=\boldsymbol{C}^{\mathrm{e}}:\left(\hat{T}+\sum_{\beta=1}^{N}\dot{\gamma}^{(\beta)}B^{(\beta)}\right) \tag{4}$$

and

$$\tau(\alpha)=(\boldsymbol{P}^{(\alpha)}+B^{(\alpha)}:\boldsymbol{C}^{\mathrm{e}}):\left(\hat{T}+\sum_{\beta=1}^{N}\dot{\gamma}^{(\beta)}B^{(\beta)}\right)=A^{(\alpha)}:\left(T+\sum_{\beta=1}^{N}\dot{\gamma}^{(\beta)}B^{(\beta)}\right), \tag{5}$$

where

$$A^{(\alpha)}=\boldsymbol{P}^{(\alpha)}+B^{(\alpha)}:\boldsymbol{C}^{\mathrm{e}}. \tag{6}$$

$\hat{T}$ is the Jaumann rate of T and $\boldsymbol{C}^{\mathrm{e}}$, the elastic compliance tensor. In eq. (5), $\sum_{\beta=1}^{N}\dot{\gamma}^{(\beta)}B^{(\beta)}$ is caused by the geometrical nonlinearity of finite deformation. Under small deformation, neglecting it does not bring about significant errors.

1 Latent hardening effect on sliding back-stress and tangent modulus

With the development of plastic deformation, critical resolved shear stress of a slip system will be updated, no matter whether the slip system is activated or not. Meanwhile, tangent moduli of activated slip systems will also be affected by the activation history of slip systems. In this paper, instantaneous critical resolved shear stress of a slip system is called its sliding back-stress, so the above phenomena are defined as back stress latent hardening and tangent modulus latent hardening (abbreviated as BSLH and TMLH hereinafter), respectively.

Micro mechanisms of BSLH are complicated. Latent hardening depends on orientations, sliding history and activated state of slip systems. When a crystal material is treated as a homogenized continuum, macro strain rate D^{p} will be a representative value of the microscopic inhomogeneous sliding. As the effect of a homogeneous strain field on a slip system in it, BSLH caused by a D^{p} should be the same; that is to say, BSLH of a slip system depends only on D^{p} and the orientation tensor of a slip system, $\boldsymbol{P}^{(\alpha)}$. There is no need to consider latent hardening effects separately for each pair of slip systems.

A slip system cannot be activated if its shear stress is within a range, bounded by two hyperplanes in the stress space. A kernel of the ranges corresponding to all of the slip systems will be the macroelastic region. When proportional limits are taken as the yield points, the evolution of subsequent yield surfaces will furnish evidence helping us infer the evolution pattern of the latent hardening law.

Experiments[5] demonstrated that subsequent yield surfaces of polycrystalline materials have three common characteristics: (i) evident Bauschinger effect — whole yield surfaces move with shape deformed during prestress; (ii) little crosseffect — the size of subsequent yield surfaces in direction perpendicular to the prestress path remains almost unchanged; (iii) evident vertex effect — there is always a high curvature area near a prestress point on subsequent yield surfaces, but the opposite part gets flatter.

All of those phenomena indicate that the sliding back-stress change rate of a slip system caused by D^p depends on the angle between $\boldsymbol{P}^{(\alpha)}$ and D^p in the stress-strain space and

$$\dot{\tau}^{(\alpha)}_{back}=\lambda \boldsymbol{P}^{(\alpha)}:D^p=\lambda\sum_{\beta=1}^{N}\dot{\gamma}^{(\beta)}\boldsymbol{P}^{(\alpha)}:\boldsymbol{P}^{(\beta)}=\lambda\sum_{\beta=1}^{N}\boldsymbol{P}_{\alpha\beta}\dot{\gamma}^{(\beta)},\ \boldsymbol{P}_{\alpha\beta}=\boldsymbol{P}^{(\alpha)}:\boldsymbol{P}^{(\beta)}, \tag{7}$$

where

$$\boldsymbol{P}_{\alpha\beta}=\boldsymbol{P}^{(\alpha)}:\boldsymbol{P}^{(\beta)} \tag{8}$$

and λ is a back-stress latent hardening modulus. Generally speaking, λ varies with the development of plastic deformation. The vertex effect will be weaker with an increase of λ. If $\lambda=0$, a sharp vertex will appear[6]. Therefore, the third characteristic can be described with an appropriate λ.

An activated criterion of a slip system can thus be formulated as

$$\begin{cases}\tau^{(\alpha)}=\tau^{(\alpha)}_{cr}\ \text{and}\ \dot{\tau}^{(\alpha)}>\dot{\tau}^{(\alpha)}_{back},\ \text{then}\ \dot{\gamma}^{(\alpha)}>0\ \text{and}\ \dot{\tau}^{(\alpha)}_{cr}=\dot{\tau}^{(\alpha)},\\ \tau^{(\alpha)}<\tau^{(\alpha)}_{cr}\ \text{or}\ \dot{\tau}^{(\alpha)}\leqslant\dot{\tau}^{(\alpha)}_{back},\ \text{then}\ \dot{\gamma}^{(\alpha)}=0\ \text{and}\ \dot{\tau}^{(\alpha)}_{cr}=\dot{\tau}^{(\alpha)}_{back}.\end{cases} \tag{9}$$

It can be easily verified that when slip systems are activated in accordance with eqs. (7) and (9), predicted subsequent yield surfaces will possess the above-mentioned three characteristics.

Resolved shear stress rate of an activated slip system should be a sum of the sliding back-stress rate and the active hardening rate, namely

$$\dot{\tau}^{(\alpha)}=\dot{\tau}^{(\alpha)}_{active}+\dot{\tau}^{(\alpha)}_{back}=h^{(\alpha)}\dot{\gamma}^{(\alpha)}+\lambda\sum_{\beta=1}^{N}P_{\alpha\beta}\dot{\gamma}^{(\beta)}, \tag{10}$$

where $h^{(\alpha)}$ is the active hardening modulus depending on self-active hardening and TMLH. From eq. (10), we know that the total hardening modulus is

$$h^{\alpha\beta}=h^{(\alpha)}\delta_{\alpha\beta}=\lambda P_{\alpha\beta}. \tag{11}$$

Substituting (11) into (9) yields a set of equations-inequalities.

$$\begin{cases} \dot{\tau}^{(\alpha)} = \sum_{\beta=1}^{N} h_{\alpha\beta}\dot{\gamma}^{(\beta)}, & \text{when } \dot{\gamma}^{(\alpha)} > 0, \\ \dot{\tau}^{(\alpha)} \leqslant \sum_{\beta=1}^{N} h_{\alpha\beta}\dot{\gamma}^{(\beta)}, & \text{when } \dot{\gamma}^{(\alpha)} = 0. \end{cases} \tag{12}$$

Eq. (12) suits all of the slip systems with $\tau=\tau_{cr}$ and can be written in matrix form

$$\begin{bmatrix} h^{(1)}+\lambda P_{11} & \lambda P_{12} & \lambda P_{13} & \lambda P_{14} & \cdots & \lambda P_{1N} \\ \lambda P_{21} & h^{(2)}+\lambda P_{22} & \lambda P_{23} & \lambda P_{24} & \cdots & \lambda P_{2N} \\ \lambda P_{31} & \lambda P_{32} & h^{(3)}+\lambda P_{33} & \lambda P_{34} & \cdots & \lambda P_{3N} \\ \lambda P_{41} & \lambda P_{42} & \lambda P_{43} & h^{(4)}+\lambda P_{44} & \cdots & \lambda P_{4N} \\ \cdots & \cdots & \cdots & \cdots & \cdots & \cdots \\ \lambda P_{N1} & \lambda P_{N2} & \lambda P_{N3} & \lambda P_{N4} & \cdots & h^{(N)}+\lambda P_{NN} \end{bmatrix} \begin{bmatrix} \dot{\gamma}^{(1)} \\ \dot{\gamma}^{(2)} \\ \dot{\gamma}^{(3)} \\ \dot{\gamma}^{(4)} \\ \cdots \\ \dot{\gamma}^{(N)} \end{bmatrix} \geqslant \begin{bmatrix} \dot{\tau}^{(1)} \\ \dot{\tau}^{(2)} \\ \dot{\tau}^{(3)} \\ \dot{\tau}^{(4)} \\ \cdots \\ \dot{\tau}^{(N)} \end{bmatrix}, \tag{13}$$

where $=$ is for slip systems with $\dot{\gamma}>0$, and $>$ for those with $\dot{\gamma}=0$. Obviously, the coefficient matrix is symmetric and positively definite.

2 Material constants and constitutive equation

Experiments demonstrate that BSLH is quite strong at the beginning of plastic deformation, and tends to be saturated gradually. In this paper, the accumulative plastic deformation is measured with the sum total of slidings

$$\Gamma = \sum_{\alpha=1}^{N} |\gamma^{(\alpha)}|, \tag{14}$$

so the evolution pattern of λ can be described by

$$\lambda = H_c e^{-\eta\Gamma} H_c e^{-\eta\left(\sum_{\alpha=1}^{N} |\gamma^{(\alpha)}|\right)}. \tag{15}$$

where H_c and η are material constants, representing the initial value of λ and its decay speed, respectively.

TMLH is assumed to follow Bassani's hardening rule[4]. Under single slip condition[3], the expression of $h^{(\alpha)}$ is

$$h^{(\alpha)} = (H_0 - H_s)\,\mathrm{sech}^2\left(\frac{H_0 - H_s}{\tau_s - \tau_0}\gamma^{(\alpha)}\right) + H_s, \tag{16}$$

where material constants H_0, H_s, τ_0 and τ_s stand for the initial and the saturate hardening modulus as well as the initial and the saturate critical strength, respectively.

Under multiple slip condition, the expression of $h^{(\alpha)}$ is

$$h^{(\alpha)} = [(H_0 - H_s)\,\mathrm{sech}^2\left(\frac{H_0 - H_s}{\tau_s - \tau_0}\ \gamma^{(\alpha)}\right) + H_s]\left[1 + \sum_{\beta=1}^{N} f_{\alpha\beta}\tanh\left(\frac{\gamma^{(\beta)}}{\gamma_0}\right)\right], \quad (f_{\alpha\alpha}=0) \tag{17}$$

where $f_{\alpha\beta}$ is the cross-hardening coefficient between the α and the β slip system, γ_0 is

another material constant reflecting the decay speed of TMLH, and $\gamma^{(\beta)}$ is the accumulative sliding of the β slip system. $f_{\alpha\beta}$ depends on the relative orientation of each pair of the 12 slip systems and has been determined by Bassani[4]. He pointed out that there are only five different values of $f_{\alpha\beta}$.

When the 12 material constants in the evolution equations of $h^{(\alpha)}$, λ and β are known, the stress-strain responses of crystal can be predicted by a constitutive equation. Since the metal crystal under large deformation is usually quite soft, an incremental constitutive equation with the compliance tensor is more suitable for numerical analysis. Substituting (5) into (12) yields

$$\begin{cases} \sum_{\beta=1}^{N} h_{\alpha\beta}\dot{\gamma}^{(\beta)} = A^{(\alpha)}:\left(\hat{T}+\sum_{\beta=1}^{N}\dot{\gamma}^{(\beta)}\boldsymbol{B}^{(\beta)}\right) & \text{when } \dot{\gamma}^{(\alpha)}>0, \\ \sum_{\beta=1}^{N} h_{\alpha\beta}\dot{\gamma}^{(\beta)} \geqslant A^{(\alpha)}:\left(\hat{T}+\sum_{\beta=1}^{N}\dot{\gamma}^{(\beta)}\boldsymbol{B}^{(\beta)}\right) & \text{when } \dot{\gamma}^{(\alpha)}=0. \end{cases} \tag{18}$$

Using notation

$$\kappa_{\alpha\beta} = h_{\alpha\beta} - A^{(\alpha)}:\boldsymbol{B}^{(\beta)} = h_{\alpha\beta} - \boldsymbol{B}^{(\alpha)}:\boldsymbol{C}^{e}:\boldsymbol{B}^{(\beta)} - \boldsymbol{P}^{(\alpha)}:\boldsymbol{B}^{(\beta)} \tag{19}$$

yields a formal result

$$\dot{\gamma}^{(\alpha)} = \left(\sum_{\beta=1}^{N}\kappa_{\alpha\beta}^{-1}A^{(\beta)}\right):\hat{T}. \tag{20}$$

Substituting (20) into (2) and (4) yields a formal incremental constitutive equation

$$D = D^{e}+D^{p} = \left(\boldsymbol{C}^{e}+\sum_{\alpha=1}^{N}\sum_{\beta=1}^{N}\kappa_{\alpha\beta}^{-1}A^{(\alpha)}\otimes A^{(\beta)}\right):\hat{T}. \tag{21}$$

It is noteworthy that though $\boldsymbol{P}^{(\alpha)}$ in (1) and $\boldsymbol{B}^{(\beta)}$ in (3) are symmetrical 2-order tensors, $\boldsymbol{P}^{(\alpha)}:\boldsymbol{B}^{(\beta)}$ is not always equal to $\boldsymbol{B}^{(\beta)}:\boldsymbol{P}^{(\alpha)}$. Generally speaking, $\kappa_{\alpha\beta}$ in (19) is not symmetrical about α and β. Moreover, (18) is a set of equations-inequalitites. It may not be easy to find $\gamma^{(\alpha)}$ directly from (18). Since (13) includes a symmetric and positive definite coefficient matrix and has one and only one solution, the solution can be obtained with the standard simplex algorithm of the linear programming theory[7] or by an iteration method. The strain-stress responses of crystal can be obtained with

$$D = D^{e}+D^{p} = \boldsymbol{C}^{e}:\left(\hat{\boldsymbol{T}}+\sum_{\alpha=1}^{N}\dot{\gamma}^{(\alpha)}\boldsymbol{B}^{(\beta)}\right)+\sum_{\alpha=1}^{N}\dot{\gamma}^{(\alpha)}\boldsymbol{P}^{(\alpha)} = \boldsymbol{C}^{e}:\hat{T}+\sum_{\alpha=1}^{N}\dot{\gamma}^{(\alpha)}A^{(\alpha)}. \tag{22}$$

3 Material constant calibration

The macro-mechanical behavior of crystal is usually measured in uniaxial tensile tests in several crystallographic orientations and the results are nominal stress-elongation curves, as shown in fig. 4. The 12 material constants are related to the stress-strain responses of crystal by complex and implicit functions. It is impossible to measure them separately in

conventional material tests. However, a good constitutive equation with appropriate material constants should well guarantee the theoretical predictions to be consistent with the experiments. Hence, the mathematical programming algorithms can be used for material constant calibration by taking the material constants as the decision variables and the deviations of theoretical predictions from experimental data as the objective function.

In uniaxial tensile tests, the stress-strain responses of crystal are sensitive to the crystallographic orientations. A number of specimens in different crystallographic orientations are required for a reliable calibration. With y_i and y_i^* ($i=1, 2, 3, \cdots, N$) denoting respectively the predicted and the measured data at the i sample point, an objective function can be defined as

$$F(x_j)=\frac{1}{2}\sum_{i=1}^{N}(y_i-y_i^*)^2, \tag{23}$$

where x_j ($j=1, 2, 3, \cdots, N$) represent the material constants.

The simplex method[8] seems inefficient for the calibration, while the steepest descent method and the variable metric methods, such as DEP and BEGS, can enable us to speed up the calibration. So we have to evaluate the gradient:

$$\frac{\partial F}{\partial x_j}=\sum_{i=1}^{N}(y_i-y_i^*)\frac{\partial y_i}{\partial x_j} \tag{24}$$

and

$$\frac{\partial^2 F}{\partial x_j \partial x_k}=\sum_{i=1}^{N}\left[\frac{\partial y_i}{\partial x_j}\frac{\partial y_i}{\partial x_k}+(y_i-y_i^*)\frac{\partial^2 y_i}{\partial x_j \partial x_k}\right]. \tag{25}$$

In eqs. (24) and (25) $\frac{\partial y_i}{\partial x_j}$ and $\frac{\partial^2 y_i}{\partial x_j \partial x_j}$ can be replaced by $\frac{\Delta y_i}{\Delta x_j}$ and $\frac{\Delta^2 y_i}{\Delta x_j \Delta x_k}$, respectively. Calculation of $\frac{\Delta^2 y_i}{\Delta x_j \Delta x_k}$ is rather tedious and the accuracy can hardly be guaranteed. If the guessed value of x_j is a good approximation, y_i can be regarded as a linear function of x_j. In this case, $\frac{\partial^2 y_i}{\partial x_j \partial x_k}=0$, so eq. (25) becomes

$$\frac{\partial^2 F}{\partial x_j \partial x_k}=\sum_{i=1}^{N}\frac{\partial y_i}{\partial x_j}\frac{\partial y_i}{\partial x_k}. \tag{26}$$

A combined algorithm of the modified Gauss-Newton method and the steepest descent method has proved very effective with the updated formula

$$\{x_k^{\text{new}}\}=\{x_k^{\text{old}}\}-\mu\left[\frac{\partial^2 F}{\partial x_i \partial x_k}+\nu\delta_{jk}\right]^{-1}\left\{\frac{\partial F}{\partial x_i}\right\}, \tag{27}$$

where μ is a coefficient selected in the search process to make $F(x_j)$ minimized in direction

$\left[\frac{\partial^2 F}{\partial x_j \partial x_k}+\nu\delta_{jk}\right]^{-1}\left\{\frac{\partial F}{\partial x_j}\right\}$, and ν is a constant to be chosen. A larger ν will make the search direction closer to the steepest descent direction. When $\nu=0$, the search direction is the same as predicted by the modified Guass-Newton method.

4 Numerical example

Figure 1 shows an FCC-crystal with 12 slip systems. Under uniaxial tests, the tensile direction corresponds to a point in the stereographic projection as illustrated in fig. 2, where '100', '010', '001' represent the x-, y-, z-directions in fig. 1. The direction cosines of '111' and '011' are $\left(\frac{\sqrt{3}}{3}, \frac{\sqrt{3}}{3}, \frac{\sqrt{3}}{3}\right)$ and $\left(0, \frac{\sqrt{2}}{2}, \frac{\sqrt{2}}{2}\right)$, respectively. There are 24 triangles in fig. 2. Because of the geometrical symmetry, we can focus our attention on the typical cases in which a tensile direction corresponds to a point in the shaded triangle[9].

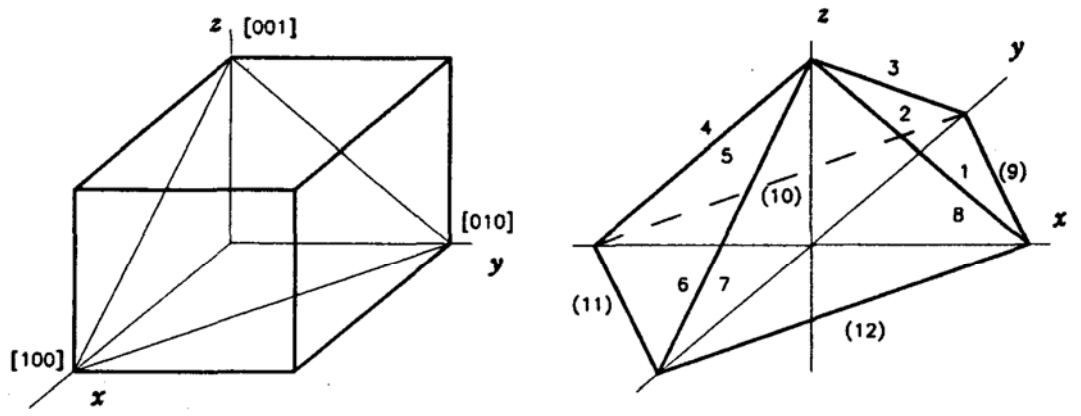

Fig. 1

The solid lines in fig. 3 are the nominal stress-elongation curves of Al-crystal simulated with material constants $\tau_s/\tau_0=2.13$, $H_0/\tau_0=21.9$, $H_s/\tau_0=2.90$, $\gamma_0=0.005$, $H_c/\tau_0=1.61$, $\eta=0.073$, $a_1=5.67$, $a_2=6.31$, $a_3=0.065$, $a_4=13.03$, $a_5=3.63$. They are in good agreement with experiments of ref. [9]. The calibration starts from a group of guessed material constants with poor predictions corresponding to the short-dashed lines in fig. 3. The long-dashed lines in fig. 3 show an intermediate result after a few iterations. The material constants listed above are the optimum values obtained at last. In the present numerical investigation, quick convergence takes place when eq. (27) is used with $\nu=0.1$—1.0.

For copper-crystal, the calibrated material constants are $\tau_s/\tau_0=2.31$, $H_0/\tau_0=36.2$, $H_s/\tau_0=3.36$, $\gamma_0=0.0017$, $H_c/\tau_0=0.76$, $\eta=0.08$, $a_1=2.38$, $a_2=2.89$, $a_3=0.38$, $a_4=23.7$, $a_5=1.14$. Fig. 4 shows that the experimental curves in ref. [10] are also well simulated.

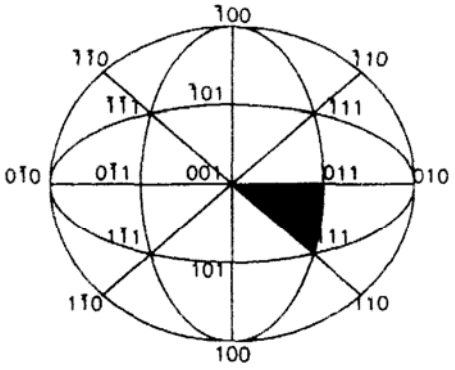

Fig. 2

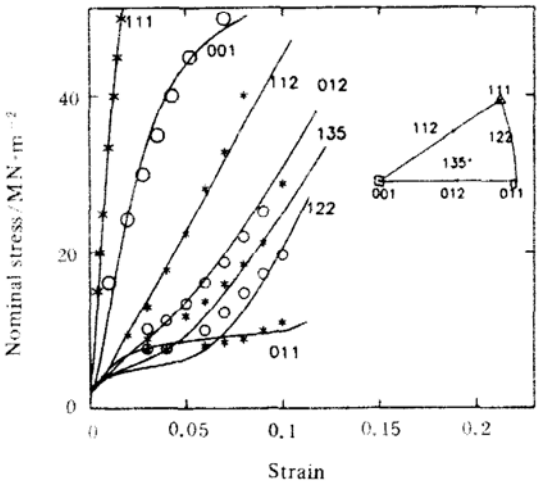

Fig. 4

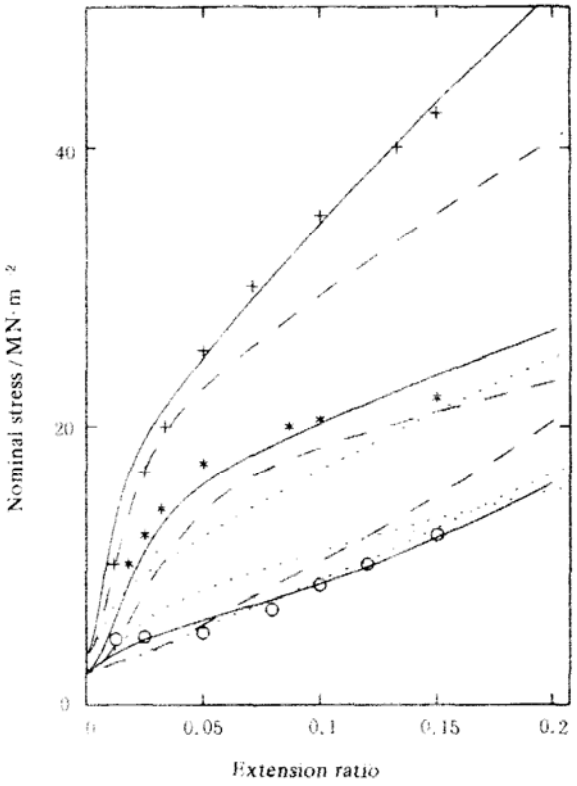

Fig. 3

These comparisons indicated that the assumptions adopted in the present work are acceptable.

5 Conclusions and discussions

1. A new expression of the crystal hardening coefficients is proposed with 12 material constants, each of which has clear physical meaning. Material constants can be determined accurately and efficiently with conventional experimental data by the suggested calibration method based on the nonlinear programming theory. The simulated load-elongation curves of the FCC crystal in tension along various crystallographic orientations are in good agreement with the experiments.

2. The hardening coefficient matrix derived from the new expression is symmetrical and positively definite, so the correct activated state and the sliding rates can be obtained with an algorithm of the mathematical programming theory.

3. There are many factors influencing the properties of crystal, whose mechanical behavior depends on the pureness, test temperature, deformation rate, etc. The new expression and the material constant calibration method proposed in this paper need to be further

verified before they are used more extensively. The experimental data in the examples are quoted from refs. [9] and [10]. In polycrystalline aggregates, impurities, defects and crystal boundaries will affect the crystal grains seriously, so the material constants may not remain the same as those in the single-crystal state, and the expression of crystal hardening coefficients should be modified as well before being extended to more general cases.

References

1 Hill, R., Generalized constitutive relations for incremental deformation of metals and crystals by multislip, *J. Mech. Phys.*, 1966, 14:95.

2 Hill, R., Rice, J. R., Constitutive analysis of elastic-plastic crystals at arbitrary strain, *J. Mech. Phys. Solid*, 1972, 20: 401.

3 Asaro, R. J., *Advances in Applied Mechanics* (eds. Hutchinson, J. W., Theodore, W. Y.), New York: Academic Press, 1983, 23:1.

4 Bassani, J. L., Single crystal hardening, *Appl. Mech. Rev.*, 1990, 43(5):320.

5 Phillips, A., Tang, J., The effect of loading path on the yield surface at elevated temperature, *Int. J. Solids Structures*, 1972, 8:463.

6 Hutchinson, J. W., Elastic-plastic behavior of polycrystalling metals and composites, *Proc. Roy. Soc.*, London, 1970, A. 319: 247.

7 Press, H. W., ed., *Numerical Recipes, the Art of Scientific Computing*, Cambridge: Cambridge University Press, 1989, 274—334.

8 Nelder, J. A., Mead, R., A simplex method for function minimization, *J. Computer*, 1965, 7:308.

9 Honeycombe, R. W. K., *The Plastic Deformation of Metals*, 2nd ed. (ed. Edward, A.), Australia, 1984, ch. 4.

10 Franciosi, P., The concepts of latent hardening and strain hardening in metallic single crystals, *Acta. Metall.*, 1985, 33(9):1 601.